JCTC Journal of Chemical Theory and Computation

Article

pubs.acs.org/JCTC

Nonlocal van der Waals Approach Merged with Double-Hybrid Density Functionals: Toward the Accurate Treatment of Noncovalent Interactions

Juan Aragó,*[,†] Enrique Ortí,[†] and Juan C. Sancho-García[‡,§]

[†]Instituto de Ciencia Molecular, Universidad de Valencia, E-46980, Spain

[‡]Departamento de Química Física, Universidad de Alicante, E-03080, Spain

[§]Laboratory of Chemistry of Novel Materials, University of Mons, B-7000, Belgium

Supporting Information

ABSTRACT: Noncovalent interactions drive the self-assembly of weakly interacting molecular systems to form supramolecular aggregates, which play a major role in nanotechnology and biochemistry. In this work, we present a thorough assessment of the performance of different double-hybrid density functionals (PBE0-DH-NL, revPBE0-DH-NL, B2PLYP-NL, and TPSS0-DH-NL), as well as their parent hybrid and (meta)GGA functionals, in combination with the most modern version of the nonlocal (NL) van der Waals correction. It is shown that this nonlocal correction can be successfully coupled with double-hybrid density functionals thanks to the short-range attenuation parameter *b*, which has been optimized against reference interaction energies of benchmarking molecular complexes (S22 and S66 databases). Among all the double-hybrid functionals evaluated, revPBE0-DH-NL and B2PLYP-NL behave remarkably accurate with mean unsigned errors (MUE) as small as 0.20 kcal/mol for the training sets and in the 0.25−0.42 kcal/mol range for an independent database (NCCE31). They can be thus seen as appropriate functionals to use in a broad number of applications where noncovalent interactions play an important role. Overall, the nonlocal van der Waals approach combined with last-generation density functionals is confirmed as an accurate and affordable computational tool for the modeling of weakly bonded molecular systems.

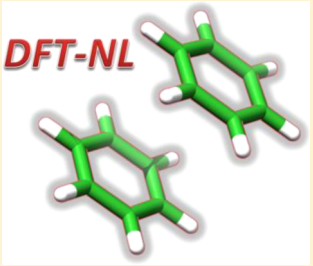

INTRODUCTION

Noncovalent interactions (NCIs) between chemical entities play a leading role for the self-assembly of molecular systems of the highest relevance for a wide variety of fields such as biochemistry and materials science.[1−4] NCIs mainly arise from long-range electron correlation effects,[5,6] which are particularly challenging, and thus, an appropriate theoretical description of these weak but important interaction forces requires highly correlated wave function methods.[7] Coupled-cluster theory with singles, doubles, and perturbatively connected triple excitations [CCSD(T)] has become the "gold-standard" method to accurately deal with these interactions in molecular systems.[2,8,9] However, its unfavorable computational $O(N^7)$ scaling, where N is related to the molecular size, prevents further applications to medium and large real-world systems without further algorithms simplifications.

Density functional theory (DFT), which is possibly by far the most widely used theory for electronic structure calculations, has a more reasonable computational cost ranging from $O(N^3)$ to $O(N^5)$. Unfortunately, standard density functionals (DFs) are unable to fully capture the long-range electron correlation phenomenon responsible for NCIs,[10−12] and thus, specific corrections need to be incorporated to make DFs as accurate as possible. Among the most modern corrections in the DFT framework, the semiempirical London-like dispersion-corrected DFT approach, originally developed by Grimme et al.[13−15] and coined in its most current version as DFT-D3, is likely to be the most popular and extended manner to theoretically treat molecular systems dominated by different types of NCIs. The DFT-D3 approximation has been widely coupled to a large number of standard DFs, from the simpler Generalized-Gradient Approximation (GGA) forms to the more sophisticated double-hybrid density functionals (DHDFs),[15] and has allowed to gain deep insight into the rich chemistry of supramolecular complexes.[16−18] In the past few years, an elegant, general, and seamless approximation, known as van der Waals density functional theory (vdW-DFT), has been also developed keeping a great interest owing to its low degree of empiricism.[19−23] The vdW-DFT approximation accounts for the long-range electron correlation phenomenon through an explicitly nonlocal (NL) correlation functional that depends only on the electron density at two different points in space ($\mathbf{r}$ and $\mathbf{r}'$) and is simply added to the general exchange-correlation energy functional. In its most modern formulation (VV10) developed by Vydrov and Van Voorhis,[24,25] this correction can be easily combined with any standard density functional after defining very few parameters entering into its formulation; this approximation is generally known as DFT-NL. Recently, Hujo and Grimme have evaluated the performance of different GGA

Received: May 1, 2013

   dx.doi.org/10.1021/ct4003527 | J. Chem. Theory Comput. XXXX, XXX, XXX−XXX

Table 1. Detailed Composition of the Exchange-Correlation Functionals Used along This Work

functional	type	$E_x[\rho]$	$E_c[\rho]$	w_{HF}[a]	w_{PT2}[b]	ref
PBE0-DH-NL	double-hybrid GGA	PBE	PBE	0.50	0.125	33
PBE0-NL	hybrid GGA	PBE	PBE	0.25	0	34, 35
PBE-NL	GGA	PBE	PBE	0	0	36
revPBE0-DH-NL	double-hybrid GGA	revPBE	revPBE	0.50	0.125	[c]
revPBE0-NL	hybrid GGA	revPBE	revPBE	0.25	0	35, 37
revPBE-NL	GGA	revPBE	revPBE	0	0	37
B2PLYP-NL	double-hybrid GGA	B88	LYP, VWN	0.53	0.27	32
B3LYP-NL	hybrid GGA	B88	LYP, VWN	0.20	0	38, 39
BLYP-NL	GGA	B88	LYP	0	0	40, 41
TPSS0-DH-NL	double-hybrid meta-GGA	TPSS	TPSS	0.50	0.125	[c]
TPSS0-NL	hybrid meta-GGA	TPSS	TPSS	0.25	0	42
TPSS-NL	meta-GGA	TPSS	TPSS	0	0	43

[a]Weight of the HF-like exchange. [b]Weight of the perturbative term. [c]This work.

and hybrid density functionals in combination with the NL correction, showing that DFT-NL can be considered as a robust and fully electronic structure method capable of dealing with the most challenging problems dominated by intermolecular NCIs.[26] Nevertheless, the NL correction has been used with only a relatively scarce number of standard DFs and needs, just like other known approaches, to be extended to more sophisticated functionals and larger molecular systems in order to become a practical and workable theoretical tool for the treatment of NCIs. DHDFs (also referred to as fifth-rung DFs according to the Perdew's scheme of "Jacob's ladder") have demonstrated to properly behave for the description of energetic and thermodynamic properties in a wide variety of different molecular systems,[27] but they still miss the efficient coupling with the NL correction.

In this paper, we hereby assess the performance of a set of double-hybrid density functionals in combination with the NL correction (PBE0-DH-NL, revPBE0-DH-NL, B2PLYP-NL, and TPSS0-DH-NL) and discuss the envisioned potential of these DHDFs to deal with weakly interacting molecular systems in a balanced way. For that purpose, we have efficiently coupled the ingredients entering into the DHDF formulation, but respecting the underlying formalism leading to every particular functional form, with the NL correction against the benchmarking S22[28,29] and S66[30,31] test sets (*vide infra*). Furthermore, a comparison with their corresponding hybrid (PBE0-NL, revPBE0-NL, B3LYP-NL, and TPSS0-NL) and (meta)GGA (PBE-NL, revPBE-NL, BLYP-NL, and TPSS-NL) functional counterparts is also done. This comparison might allow to gain more insight concerning the dependence of the NL correction on the nature of the density functional across the whole hierarchy of methods and to get a complete picture of the performance of existing possibilities: pure, hybrid, and double-hybrid DFT-based approaches. Finally, we analyze the performance of the different density functionals with respect to the type of overriding noncovalent interaction (hydrogen bonds, dispersion interactions, and mixed interactions) offering some clues regarding the behavior of a density functional corrected with the NL approach.

THEORETICAL MODELS AND COMPUTATIONAL DETAILS

Four different models of DFs have been employed in this work. Note that the (meta)Generalized-Gradient Approximation (GGA) is treated as the baseline for further improvements (rungs) within each family. A general expression for the exchange-correlation (xc) functionals utilized is as follows:

$$E_{xc}[\rho] = w_{HF}E_x^{HF} + (1 - w_{HF})E_x[\rho] + w_{PT2}E_c^{PT2} + (1 - w_{PT2})E_c[\rho] + E_c^{NL}[\rho] \quad (1)$$

where $E_x[\rho]$ and $E_c[\rho]$ correspond to the (meta)GGA exchange and correlation energy terms, respectively, weighted by the respective w_i value. E_x^{HF} and E_c^{PT2} are, respectively, the exact exchange HF-like energy and the correlation energy obtained at the Møller−Plesset perturbation theory up to second order.[32] Note that the E_x^{HF} and E_c^{PT2} terms are evaluated here with the orbitals arising from the solution of the Kohn−Sham one-electron equations but discarding the perturbative term. Table 1 presents the detailed composition of all the exchange-correlation functionals used in this work.

E_c^{NL} is the NL correlation term, which is added to the exchange-correlation energy functional non self-consistently, although this is not expected to significantly influence the results.[26] In the DFT-NL approach proposed by Vydrov and Van Voorhis, the E_c^{NL} functional is formulated as

$$E_c^{NL}[\rho] = \int d\mathbf{r}\rho(\mathbf{r})\left[\beta(b) + \frac{1}{2}\int d\mathbf{r}'\rho(\mathbf{r}')\Phi(\mathbf{r},\mathbf{r}')\right] \quad (2)$$

where ρ is the total electron density, while the kernel function $\Phi(\mathbf{r},\mathbf{r}')$ and $\beta(b)$ are defined as follows (in atomic units):

$$\Phi(\mathbf{r},\mathbf{r}') = -\frac{3}{2gg'(g+g')}, \qquad g = \omega_0(\mathbf{r})R^2 + \kappa(\mathbf{r}),$$
$$g' = \omega_0(\mathbf{r}')R^2 + \kappa(\mathbf{r}'), \qquad R = |\mathbf{r} - \mathbf{r}'|,$$
$$\omega_0(\mathbf{r}) = \sqrt{C\left|\frac{\nabla\rho(\mathbf{r})}{\rho(\mathbf{r})}\right|^4 + \frac{4\pi}{3}\rho(\mathbf{r})},$$
$$\kappa(\mathbf{r}) = b\frac{3\pi}{2}\left[\frac{\rho(\mathbf{r})}{9\pi}\right]^{1/6}, \qquad \beta(b) = \frac{1}{32}\left[\frac{3}{b^2}\right]^{3/4} \quad (3)$$

the adjustable parameter b controls the short-range damping of the R^{-6} asymptote and prevents the double-counting of correlation energy effects at the short-range region; we refer to the original work for further details.[24] The short-range attenuation parameter b is carefully fitted here to the S22[28,29] and S66[30,31] data sets, whereas the long-range parameter C is fixed to its original value ($C = 0.0093$), since it has been demonstrated that its optimization leads to only minor improvements.[26] The S22 and S66 databases collect reference

dx.doi.org/10.1021/ct4003527 | J. Chem. Theory Comput. XXXX, XXX, XXX−XXX

Table 2. Optimized Short-Range Attenuation Parameter (b), as well as ME (kcal/mol), MUE (kcal/mol), and MURE (%) Computed for the S22 and S66 Noncovalent Interaction Benchmarking Sets at the DFT-NL/def2-QZVP Level[a]

	S22				S66			
functional	b	ME	MUE	MURE	b	ME	MUE	MURE
PBE0-DH		1.57	1.66	36.7		1.46	1.49	41.4
PBE0		2.31	2.36	52.2		2.01	2.02	55.2
B2PLYP		1.91	1.91	43.0		1.72	1.72	46.3
B3LYP		3.77	3.77	85.8		3.25	3.25	86.4
PBE0-DH-NL	8.6	−0.32	0.46	7.0	8.3	−0.24	0.33	5.3
PBE0-NL	6.5	−0.38	0.54	8.2	6.6	−0.27	0.38	6.2
PBE-NL	6.2	−0.34	0.48	7.6	6.5	−0.21	0.40	7.1
revPBE0-DH-NL	6.0	−0.03	0.19	4.0	5.7	−0.04	0.19	4.1
revPBE0-NL	4.3[b]		0.18[b]		4.2	−0.02	0.16	3.3
revPBE-NL	3.7[b]		0.29[b]		3.6	−0.04	0.20	4.6
B2PLYP-NL	8.3	−0.06	0.21	4.0	7.8	−0.12	0.20	3.6
B3LYP-NL	4.8[b]		0.48[b]		4.6	−0.24	0.34	5.3
BLYP-NL	4.0[b]		0.40[b]		4.0	−0.04	0.30	6.2
TPSS0-DH-NL	7.1	−0.26	0.41	5.8	6.8	−0.18	0.31	5.2
TPSS0-NL	5.4	−0.29	0.46	6.2	5.2	−0.25	0.33	5.1
TPSS-NL	5.0	−0.23	0.43	6.3	5.0	−0.11	0.34	6.2

[a]ME, MUE, and MURE errors computed for PBE0, PBE0-DH, B3LYP, and B2PLYP are also included for comparison purposes. [b]Values taken from ref 26.

interaction energies calculated at the 'gold-standard' CCSD(T) level with large enough basis sets and are thus widely used to calibrate and assess newly developed computational methods. These S22 and S66 test sets cover a large number of weakly bonded molecular complexes dominated by hydrogen bonds, dispersion interactions, and mixed interactions (hydrogen bonds and dispersion). The molecular structures for the S22 and S66 sets are taken from refs 28 and 30, respectively, whereas the reference interactions energies are taken from the most updated revisions (refs 29 and 31 for S22 and S66, respectively). To assess the errors of the different DFT-NL functionals, the mean signed error (ME), mean unsigned error (MUE), and mean unsigned relative error (MURE) are employed. A negative ME indicates an overbinding trend, while positive ME values in the interaction energies signify underbinding.

The ORCA program[44] and the def2-QZVP basis set, which is known to provide results sufficiently close to the basis set limit, were used for all calculations. Therefore, the Basis Set Superposition Error (BSSE) is expected to be negligible, and consequently, the intermolecular interaction energies are not counterpoise corrected. Note that the counterpoise method to estimate the BSSE is believed to overestimate this effect, and some authors even propose to scale it down by half of its value.[45] The computational effort is significantly reduced in all cases by making use of the 'resolution of the identity' (RI)[46] and the 'chain-of-spheres' (COSX)[47] techniques, for Coulomb or exchange integrals, respectively, using for them the corresponding matching auxiliary basis sets.[48] The quadrature grids needed for numerical integration of DFs are also increased with respect to defaults, which is strongly recommended for intermolecular interaction energies, as well as the corresponding thresholds for converging energies self-consistently.

RESULTS AND DISCCUSSION

To evaluate the performance of the different DFs utilized in combination with the NL approach, the short-range attenuation parameter b needs to be first defined. Table 2 summarizes the optimum values found as well as the corresponding ME, MUE, and MURE errors calculated for interaction energies (S22 and S66 databases) with respect to the reference data.[29,31] The variation of the MUE error with b for each DFT-NL functional, as well as the interaction energies of the weakly bonded molecular complexes computed at its optimized b parameter, are given in the Supporting Information. Table 2 shows how the short-range attenuation parameter b does not depend too much on the data set employed. This dependence is, however, slightly more pronounced for DHDFs; for instance, the attenuation parameter b calculated for PBE0-DH-NL varies from 8.6 to 8.3 when passing from the S22 test set to S66. The same trend is found for the rest of DHDFs assessed (Table 2). Additionally, keeping the same value of the attenuation parameter b (see, for instance, the case of BLYP-NL and TPSS-NL in Table 2), MUEs are smaller for S66 than for S22. Note that the S66 database has been expressly built to be more complete than the previously designed S22 test set due to the incorporation of a larger number of representative weakly bonded molecular complexes,[30] and therefore, only the results obtained for the S66 test set will be hereafter discussed.

Besides this, a dependence on the short-range attenuation parameter b with the nature of the density functional is clearly evidenced in Table 2. DHDFs always exhibit the largest value for b within a density functional family. This finding can be easily understood if the expression where the short-range attenuation parameter b appears is closely analyzed (eq 3). As mentioned, b mostly controls the portion of the E_c^{NL} energy at short regions, and therefore, DHDFs, which already incorporate some nonlocal correlation effects through the perturbative term, need larger values for b to significantly reduce the amount of the correlation energy that comes from the E_c^{NL} term, thereby avoiding undesired double-counting of correlation energy. Among the different DHDFs evaluated, PBE0-DH-NL is the density functional with the largest b (8.3) followed by B2PLYP-NL (7.8), TPSS0-DH-NL (6.8), and revPBE0-DH-NL (5.7). Interestingly, the difference between the values of the attenuation parameter b for a determined DHDF and its hybrid-(meta)GGA homologous is quite similar (1.4−1.7), except for the B2PLYP-NL family, where the difference of b

dx.doi.org/10.1021/ct4003527 | J. Chem. Theory Comput. XXXX, XXX, XXX−XXX

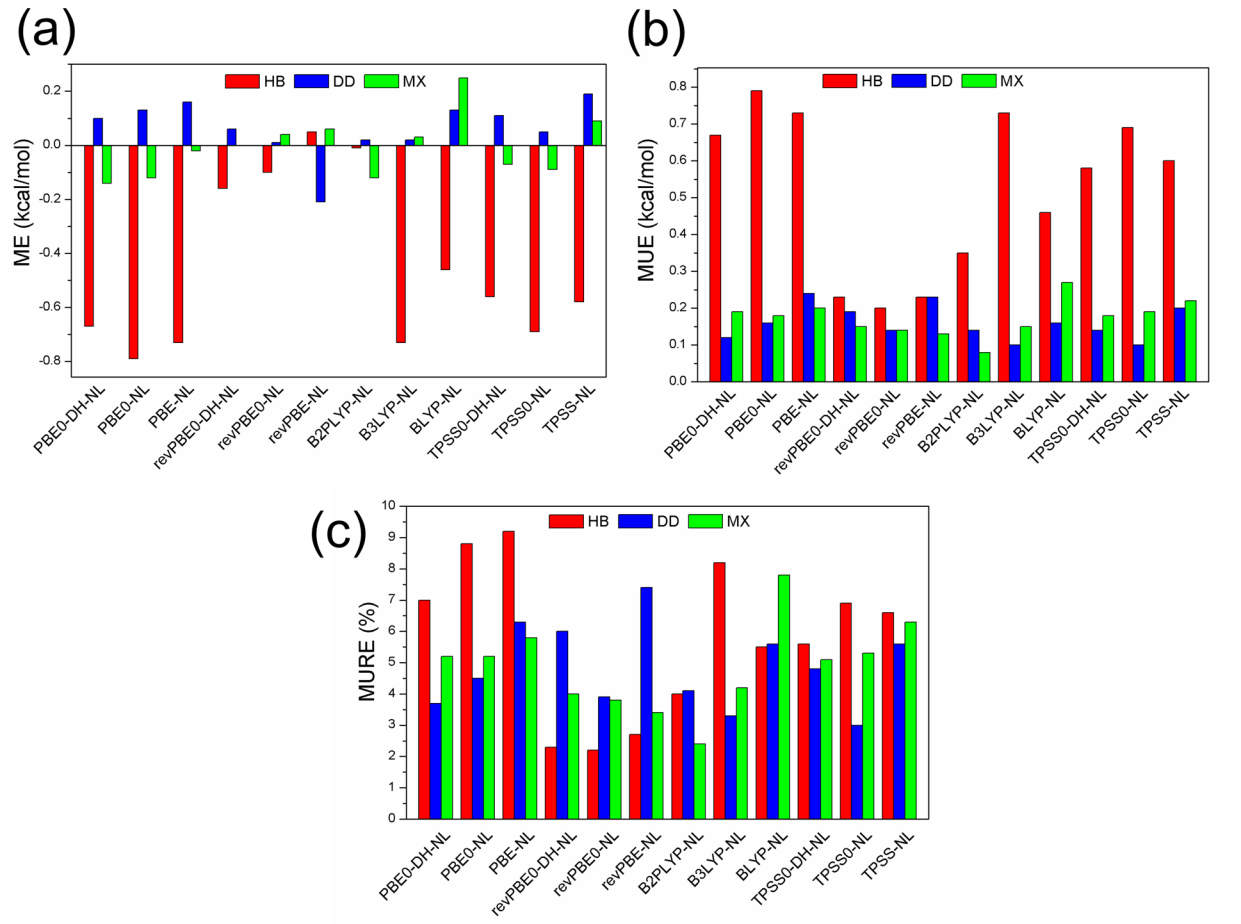

Figure 1. ME (a), MUE (b), and MURE (c). Values computed for the three groups of molecular complexes: hydrogen-bonded (red), London dispersion-dominated (blue), and "mixed" complexes (green) within the S66 test set.

with respect to the B3LYP-NL functional rises to 3.2. The values of *b* obtained for the hybrid-(meta)GGA and (meta)-GGA DFs are rather similar, with differences ranging from 0.1 (PBE0-NL vs PBE-NL) to 0.6 (revPBE0-NL vs revPBE-NL and B3LYP-NL vs BLYP-NL).

Overall, and most importantly, a close inspection of Table 2 reveals that DHDFs exhibit the best performance within a family of DFs providing the smallest MUE and MURE errors. For instance, within the PBE density functional family, the MUE value noticeably decreases from 0.40 kcal/mol (PBE-NL) to 0.38 kcal/mol (PBE0-NL) and to 0.33 kcal/mol (PBE0-DH-NL). In terms of performance, the revPBE0-DH-NL and B2PLYP-NL functionals provide interaction energies very close to the reference values with low MUE of 0.19 and 0.20 kcal/mol, respectively. Note that the MUE values computed for these DFT-NL functionals are slightly smaller than those reported for other similar double-hybrid density functionals within the DFT-D3 scheme (e.g., 0.26 kcal/mol for B2PLYP-D3).[49] For comparison purposes, the ME, MUE, and MURE errors computed for the double-hybrid (PBE0-DH and B2PLYP) and the hybrid (PBE0 and B3LYP) functionals for S22 and S66 have been also included in Table 2. The MUE values are above of 1.5 kcal/mol for all standard functionals evaluated.

Regarding the (meta)GGA and hybrid functionals, MUE values are similar within a density functional family and are in the 0.30−0.40 kcal/mol range with the exception of the revPBE-NL (GGA) and revPBE0-NL (hybrid) functionals, which display MUE values in the 0.16−0.20 kcal/mol range (Table 2). Indeed, revPBE-NL and revPBE0-NL show an excellent performance at a reasonable computational cost, and the hybrid revPBE0-NL functional presents the smallest MUE value (0.16 kcal/mol) among all the density functionals assessed. This finding is in agreement with the results obtained by Hujo and Grimme,[26] where revPBE0-NL was also proven to behave as an appropriate density functional to describe NCIs in an accurate way. The MUE values computed for both revPBE-NL (0.20 kcal/mol) and revPBE0-NL (0.16 kcal/mol) in this work are slightly smaller than those found by Hujo and Grimme (0.21 and 0.24 kcal/mol, respectively). The discrepancy might be caused by the difference in the optimization of the *b* parameter (taken from S66 instead of S22) and mainly by the difference in the adopted reference values for the S66 test set. The small MUE value calculated for revPBE0-NL is totally comparable with that found for the LC-VV10 functional (0.15 kcal/mol),[50] which is, as far as we know, the smallest MUE found within the DFT framework. It should be also stressed that the MUE values computed for revPBE-NL and revPBE0-NL are slightly smaller than those calculated with the pairwise revPBE-D3 (0.31 kcal/mol) and revPBE0-D3 (0.22 kcal/mol) approaches.[49]

The ME, MUE, and MURE values computed for the hydrogen-bonded, London dispersion-dominated, and "mixed" complexes of the S66 data set are displayed in Figure 1. A general trend for most of the DFs assessed is the over-estimation of the interaction energies in hydrogen-bonded

dx.doi.org/10.1021/ct4003527 | J. Chem. Theory Comput. XXXX, XXX, XXX−XXX

molecular complexes with negative MEs (Figure 1a). The revPBE-NL functional is the only one that deviates from this trend underbinding the interaction energy for hydrogen-bonded complexes. Additionally, this class of molecular complexes presents the largest MUEs, above 0.40 kcal/mol for eight out of the twelve density functionals used (Figure 1b). According to the MUE values, the revPBE-based and B2PLYP-NL functionals provide the best performance for the hydrogen-bonded complexes subset of the S66 data set. It should be noted that, notwithstanding the large MUEs, the MURE error, which is a more stringent criterion, is found in the 2.2−9.2% range for all DFs evaluated (Figure 1c). The smallest MUREs are computed for the revPBE family (2.2−2.7%), whereas the largest MUREs are calculated for the PBE family (7.0−9.2%).

For the London dispersion-dominated complexes, an underbinding (positive MEs) of the interaction energies is obtained with respect to the reference values for most functionals investigated; the exception being again the case of revPBE-NL, which now overestimates the binding energies (Figure 1a). For this subset, the DFT-NL functionals have turned out to behave superbly with MUEs below 0.25 kcal/mol (Figure 1b). Note that all DHDFs exhibit MUEs around 0.14 kcal/mol. Nevertheless, the hybrid B3LYP-NL and TPSS0-NL functionals present the best performance with MUE values as small as 0.10 kcal/mol. The MURE values computed for the different DFs range from 3.0 to 7.4%, and the smallest MURE is found for the TPSS0-NL functional, while revPBE-NL displays the largest MURE (Figure 1c).

For the complexes dominated by "mixed" interactions, we do not find any systematic trend concerning the overbinding or underbinding of the interaction energies (Figure 1a). In general, the MUE values computed for these "mixed" complexes are similar to those obtained for the London dispersion-dominated complexes (Figure 1b) with values in the 0.08−0.27 kcal/mol range. In this S66 subset, the double-hybrid B2PLYP-NL performs excellently with a MUE (MURE) value of 0.08 kcal/mol (2.4%), whereas the GGA BLYP-NL functional, which belongs to the same family, presents the largest deviation with a MUE (MURE) value of 0.27 kcal/mol (7.8%). A closer inspection of Figure 1c reveals that, despite their relative large total MURE errors, the double-hybrid TPSS0-DH-NL and the meta-GGA TPSS-NL functionals show a small dispersion of MURE values between the S66 subsets. This clearly highlights the robustness of these DFs to describe weakly bound molecular complexes of different nature on equal footing.

In a further step, a cross-validation process to assess the performance of the best DHDF functionals merged with the NL correction (revPBE0-DH-NL and B2PLYP-NL) using an independent database (i.e., a database that has not been employed for the optimization of the parameter b) has been carried out. The values for the parameter b employed for each density functional are those previously optimized for S66. The database selected is named NCCE31[51,52] and comprises five subsets: six hydrogen-bonded (HB6), seven charge-transfer (CT7), six dipole interaction (DI6), seven weak interaction (WI7), and, finally, five $\pi-\pi$ stacking (PPS5) complexes. The NCCE31 database collects reference interaction energies calculated at the 'gold-standard' CCSD(T) level with large enough basis sets and can be used to assess the performance of newly developed computational methods.

Table 3 summarizes the ME, MUE, and MURE errors obtained for the interaction energies calculated for the NCCE31 database with respect to the reference data.[51,52] A close inspection of Table 3 reveals that DHDFs exhibit the best behavior within a family of DFs providing the smallest MUE and MURE errors. For instance, the MUE value notably decreases from 0.93 kcal/mol (revPBE-NL), to 0.41 kcal/mol (revPBE0-NL), and to 0.25 kcal/mol (revPBE0-DH-NL). The same trend is found for the B2PLYP-NL density functional family, for which the MUE values are 1.12, 0.77, and 0.42 kcal/mol for BLYP-NL, B3LYP-NL, and B2PLYP-NL, respectively. The comparison of the MUE values for the S66 database with those obtained for NCCE31 (Table 2 and Table 3) indicates that DHDFs coupled with the NL correction are more robust than their parent hybrid and GGA functionals to describe weakly interacting molecular complexes. For revPBE0-DH-NL, MUE undergoes a slight deviation from 0.19 kcal/mol (S66) to 0.25 kcal/mol (NCCE31). In contrast, for revPBE0 (revPBE), MUE values notably increase from 0.16 (0.20) to 0.41 (0.93) kcal/mol when passing from S66 to NCCE31, respectively. The MUE deviations between S66 and NCCE31 for the B2PLYP-NL density functional family are even more accentuated (Tables 2 and 3). These findings computed for an independent database (NCCE31) highlight that, despite their higher computational cost, DHDFs merged with the NL correction provide an accurate description of supramolecular complexes even in systems beyond the training sets.

Table 3. ME (kcal/mol), MUE (kcal/mol), and MURE (%) Computed for the NCCE31 Noncovalent Interaction Benchmarking Set at the DFT-NL/def2-QZVP Level

	NCCE31			
functional	b	ME	MUE	MURE
revPBE0-DH-NL	5.7	−0.15	0.25	16.4
revPBE0-NL	4.2	−0.37	0.41	20.3
revPBE-NL	3.6	−0.90	0.93	46.0
B2PLYP-NL	7.8	−0.35	0.42	14.5
B3LYP-NL	4.6	−0.69	0.77	26.3
BLYP-NL	4.0	−0.99	1.12	47.0

An aspect that deserves further attention is the behavior of DHDFs merged with the NL correction at long-range distances. Note that parameter C, which mainly controls the long-range region, was fixed to its original value (C = 0.0093). This parameter was fitted to provide accurate asymptotic molecular dispersion coefficients for a GGA (VV10) functional.[24] Since DHDFs are able to partially capture nonlocal correlation effects through the perturbative term even at the long-range region, a possible overestimation of van der Waals interactions in the long-range might take place. In an attempt to mitigate the possible overestimation at long-range distances, parameter C has been slightly modified to diminish the nonlocal correlation term. To investigate the effect of this change, B2PLYP-NL/def2-QZVP potential energy curves have been computed for the parallel-displaced benzene−benzene dimer by increasing parameter C up to 10% starting from its original value. The interaction energies computed using different values of C are very similar with deviations smaller than 0.003 kcal/mol at long-range distances (Figure S3, Supporting Information) and the increase of C is therefore found to have a negligible effect on the tail of the potential energy curve. Thus, the parametrization of b maintaining fixed C as performed above appears to be reasonable.

To explore in more detail the possible overestimation of the van der Waals interactions in the long-range, potential energy

dx.doi.org/10.1021/ct4003527 | J. Chem. Theory Comput. XXXX, XXX, XXX−XXX

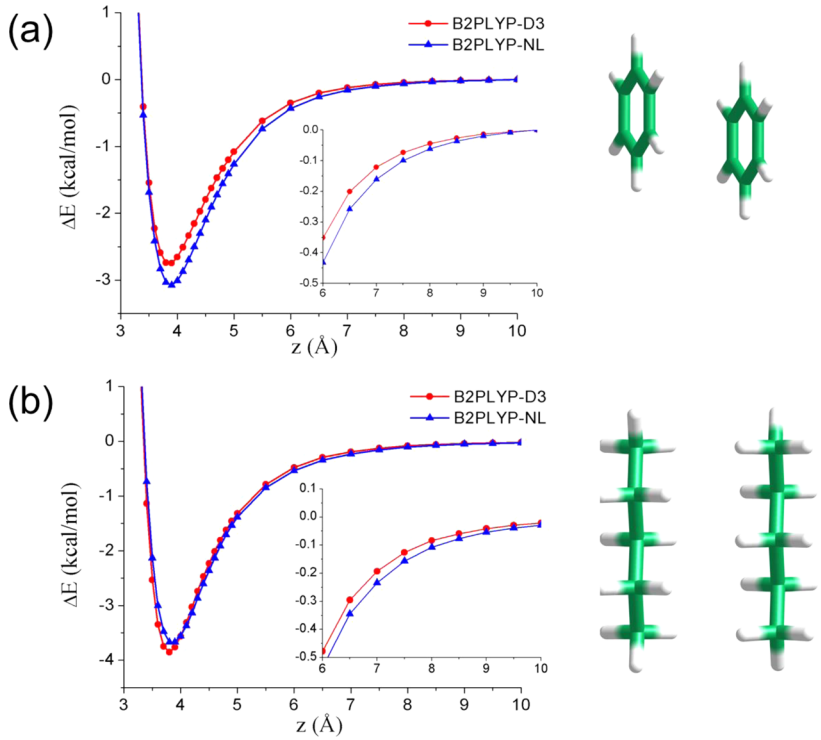

Figure 2. Potential energy curves computed for the parallel-displaced benzene−benzene (a) and pentane−pentane (b) dimers at the B2PLYP-D3 and B2PLYP-NL (b = 7.8) level using the def2-QZVP basis set.

curves for the parallel-displaced benzene−benzene and pentane−pentane dimers at the B2PLYP-D3 and B2PLYP-NL level using the def2-QZVP basis set have been computed. The B2PLYP-NL functional was employed with the previously optimized parameter b (7.8) for S66. Note that B2PLYP-D3 is specially corrected (the parameter S_6 is smaller than 1; see ref 15 for details) to compensate the amount of correlation energy provided by the perturbative term. Potential energy curves were constructed by plotting the intermolecular interaction energy between the two monomers and by varying the distance between the mass centers along the z axis. It should be noted that the parallel-displaced benzene−benzene and pentane−pentane dimers have been selected because they present a large molecular size within the S66 database, and thus, the overestimation is expected to be larger for these dimers. The potential energy curves shown in Figure 2 clearly reveal that the overestimation of the interaction energy obtained for the B2PLYP-NL functional compared to B2PLYP-D3 at long-range distances (>7 Å) is rather small with deviations smaller than 0.04 kcal/mol for both dimers. This small deviation might not be only associated to the perturbative term, since it has been already shown that the estimated accuracy for asymptotic molecular dispersion coefficients is slightly worse for NL than D3.[26] These results furthermore demonstrate that DHDFs, once the parameter b has been thoroughly optimized, are able to give a reasonable description for weakly bonded complexes even in the long-range regions where they have not been specially adapted.

CONCLUSIONS

In this contribution, we have thoroughly assessed the performance of a variety of double-hybrid density functionals, as well as their hybrid and (meta)GGA counterparts, in combination with the nonlocal van der Waals correction formulated by Vydrov and Voorhis to deal with weakly interacting molecular systems dominated by noncovalent interactions. The results clearly highlight that the nonlocal correction can be successfully employed with double-hybrid density functionals once the short-range attenuation parameter b, which avoids double-counting of correlation energy at short interacting electronic distances, is carefully fitted. Among the double-hybrid functionals evaluated, revPBE0-DH-NL and B2PLYP-NL behave remarkably accurate with mean unsigned errors around 0.20 kcal/mol for the training sets (S22 and S66) and in the 0.25−0.42 kcal/mol range for an independent database (NCCE31). Thus, these double hybrid density functionals can be seen as appropriate functionals to be used in a broad number of chemical applications involving noncovalent interactions. We remain optimistic about the accuracy and generality of the nonlocal van der Waals approach combined with standard density functionals for reliable studies in supramolecular chemistry.

ASSOCIATED CONTENT

Supporting Information

Variation of the MUE error with the attenuation parameter b for each DFT-NL functional and interaction energies computed with the optimized b parameter for the weakly bonded molecular complexes. This material is available free of charge via the Internet at http://pubs.acs.org.

AUTHOR INFORMATION

Corresponding Author

*E-mail: juan.arago@uv.es.

Notes

The authors declare no competing financial interest.

■ ACKNOWLEDGMENTS

Financial support by the "Ministerio de Economía y Competitividad" (MINECO) of Spain and the "European Regional Development Fund" through projects CTQ2011-27253, CTQ2012-31914, and Consolider-Ingenio CSD2007-00010 in Molecular Nanoscience is acknowledged. The support of the Generalitat Valenciana (Prometeo/2012/053) is also acknowledged. J.C.S.G. holds a visiting professorship (University of Mons) founded by the Belgian National Fund of Scientific Research (FNRS).

■ REFERENCES

(1) Riley, K. E.; Hobza, P. *Acc. Chem. Res.* **2013**, *46*, 927−936.
(2) Riley, K. E.; Hobza, P. *WIREs Comput. Mol. Sci.* **2011**, *1*, 3−17.
(3) González-Rodríguez, D.; Schenning, A. P. H. J. *Chem. Mater.* **2010**, *23*, 310−325.
(4) Kulkarni, C.; Balasubramanian, S.; George, S. J. *ChemPhysChem* **2013**, *14*, 661−673.
(5) Stone, A. J. *The Theory of Intermolecular Forces*; Oxford University Press: New York, 1997; p 50−63.
(6) Kaplan, I. G. *Intermolecular Interactions: Physical Picture, Computational Methods and Model Potentials*; John Wiley & Sons: Chichester, 2006; p 44−50.
(7) Hohenstein, E. G.; Sherrill, C. D. *WIREs Comput. Mol. Sci.* **2012**, *2*, 304−326.
(8) Riley, K. E.; Pitonak, M.; Jurecka, P.; Hobza, P. *Chem. Rev.* **2010**, *110*, 5023−5063.
(9) Hobza, P. *Acc. Chem. Res.* **2012**, *45*, 663−672.
(10) Kristyán, S.; Pulay, P. *Chem. Phys. Lett.* **1994**, *229*, 175−180.
(11) Hobza, P.; šponer, J.; Reschel, T. *J. Comput. Chem.* **1995**, *16*, 1315−1325.
(12) Allen, M. J.; Tozer, D. J. *J. Chem. Phys.* **2002**, *117*, 11113−11120.
(13) Grimme, S. *J. Comput. Chem.* **2004**, *25*, 1463−1473.
(14) Grimme, S. *J. Comput. Chem.* **2006**, *27*, 1787−1799.
(15) Grimme, S.; Antony, J.; Ehrlich, S.; Krieg, H. *J. Chem. Phys.* **2010**, *132*, 154104.
(16) Grimme, S. *Chem.—Eur. J.* **2012**, *18*, 9955−9964.
(17) Risthaus, T.; Grimme, S. *J. Chem. Theory Comput.* **2013**, *9*, 1580−1591.
(18) Waller, M. P.; Kruse, H.; Muck-Lichtenfeld, C.; Grimme, S. *Chem. Soc. Rev.* **2012**, *41*, 3119−3128.
(19) Dion, M.; Rydberg, H.; Schröder, E.; Langreth, D. C.; Lundqvist, B. I. *Phys. Rev. Lett.* **2004**, *92*, 246401.
(20) Lee, K.; Murray, É. D.; Kong, L.; Lundqvist, B. I.; Langreth, D. C. *Phys. Rev. B* **2010**, *82*, 081101.
(21) Vydrov, O. A.; Van Voorhis, T. *Phys. Rev. Lett.* **2009**, *103*, 063004.
(22) Vydrov, O. A.; Voorhis, T. V. *J. Chem. Phys.* **2009**, *130*, 104105.
(23) Vydrov, O. A.; Van Voorhis, T. *Phys. Rev. A* **2010**, *81*, 062708.
(24) Vydrov, O. A.; Voorhis, T. V. *J. Chem. Phys.* **2010**, *133*, 244103.
(25) Vydrov, O. A.; Voorhis, T. V. *J. Chem. Phys.* **2010**, *132*, 164113.
(26) Hujo, W.; Grimme, S. *J. Chem. Theory Comput.* **2011**, *7*, 3866−3871.
(27) Goerigk, L.; Grimme, S. *J. Chem. Theory Comput.* **2010**, *7*, 291−309.
(28) Jurecka, P.; Sponer, J.; Cerny, J.; Hobza, P. *Phys. Chem. Chem. Phys.* **2006**, *8*, 1985−1993.
(29) MCarshall, M. S.; Burns, L. A.; Sherrill, C. D. *J. Chem. Phys.* **2011**, *135*, 194102.
(30) Řezáč, J.; Riley, K. E.; Hobza, P. *J. Chem. Theory Comput.* **2011**, *7*, 2427−2438.
(31) Řezáč, J.; Riley, K. E.; Hobza, P. *J. Chem. Theory Comput.* **2011**, *7*, 3466−3470.
(32) Grimme, S. *J. Chem. Phys.* **2006**, *124*, 034108−034116.
(33) Bremond, E.; Adamo, C. *J. Chem. Phys.* **2011**, *135*, 024106.
(34) Ernzerhof, M.; Scuseria, G. E. *J. Chem. Phys.* **1999**, *110*, 5029−5036.
(35) Adamo, C.; Barone, V. *J. Chem. Phys.* **1999**, *110*, 6158−6170.
(36) Perdew, J. P.; Burke, K.; Ernzerhof, M. *Phys. Rev. Lett.* **1996**, *77*, 3865−3868.
(37) Zhang, Y.; Yang, W. *Phys. Rev. Lett.* **1998**, *80*, 890−890.
(38) Becke, A. D. *J. Chem. Phys.* **1993**, *98*, 5648−5652.
(39) Barone, V.; Adamo, C. *Chem. Phys. Lett.* **1994**, *224*, 432−438.
(40) Becke, A. D. *Phys. Rev. A* **1988**, *38*, 3098−3100.
(41) Lee, C.; Yang, W.; Parr, R. G. *Phys. Rev. B* **1988**, *37*, 785−789.
(42) Sancho-Garcia, J. C. *J. Chem. Phys.* **2006**, *124*, 124112.
(43) Tao, J.; Perdew, J. P.; Staroverov, V. N.; Scuseria, G. E. *Phys. Rev. Lett.* **2003**, *91*, 146401.
(44) Neese, F. *WIREs Comput. Mol. Sci.* **2012**, *2*, 73−78.
(45) Kruse, H.; Grimme, S. *J. Chem. Phys.* **2012**, *136*, 154101.
(46) Eichkorn, K.; Treutler, O.; Öhm, H.; Häser, M.; Ahlrichs, R. *Chem. Phys. Lett.* **1995**, *240*, 283−290.
(47) Neese, F.; Wennmohs, F.; Hansen, A.; Becker, U. *Chem. Phys.* **2009**, *356*, 98−109.
(48) Eichkorn, K.; Weigend, F.; Treutler, O.; Ahlrichs, R. *Theor. Chem. Acc.* **1997**, *97*, 119−124.
(49) Goerigk, L.; Kruse, H.; Grimme, S. *ChemPhysChem* **2011**, *12*, 3421−3433.
(50) Vydrov, O. A.; Van Voorhis, T. *J. Chem. Theory Comput.* **2012**, *8*, 1929−1934.
(51) Zhao, Y.; Truhlar, D. G. *J. Phys. Chem. A* **2005**, *109*, 5656−5667.
(52) Zhao, Y.; Truhlar, D. G. *J. Chem. Theory Comput.* **2005**, *1*, 415−432.